

LASER POWERED LAUNCH VEHICLE PERFORMANCE ANALYSES

Final Technical Report

Order Number: H-32385D

Prepared for

**National Aeronautics and Space Administration
George C. Marshall Space Flight Center
Marshall Space Flight Center, AL 35812**

by

Y. S. Chen
J. Liu

**Engineering Sciences, Inc.
1900 Golf Road, Suite D
Huntsville, AL 35802
(256) 883-6233**

August 31, 2001

LASER POWERED LAUNCH VEHICLE PERFORMANCE ANALYSES

OBJECTIVES

The purpose of this study is to establish the technical ground for modeling the physics of laser powered pulse detonation phenomenon. Laser powered propulsion systems involve complex fluid dynamics, thermodynamics and radiative transfer processes. Successful predictions of the performance of laser powered launch vehicle concepts depend on the sophisticated models that reflect the underlying flow physics including the laser ray tracing the focusing, inverse Bremsstrahlung (IB) effects, finite-rate air chemistry, thermal non-equilibrium, plasma radiation and detonation wave propagation, etc. The proposed work will extend the base-line numerical model to an efficient design analysis tool. The proposed model is suitable for 3-D analysis using parallel computing methods. The technical objectives of the present project are:

1. Extend the laser propulsion analysis model to 3-D applications.
2. Develop the laser ray-tracing model and laser-focusing model suitable for general 3-D geometry conditions.
3. Implement the efficient treatment for modeling the plasma radiation model such that it can be ready for 3-D applications.
4. Investigate the laser ignition process and its effects on the launch vehicle performance.
5. Develop the ray-tracing and radiation model to be suitable for parallel computing environment.
6. Investigate the air-breathing and rocket modes modeling effects.

INTRODUCTION

Currently, NASA's aim of operating low cost launch and space vehicles requires the research and development of advanced propulsion technologies and concepts. One plausible advanced concept is the utilization of off-board pulsed laser power source to propel small payload (e.g. 100kg) into earth orbit. The merit of the laser-propelled vehicles is in its high efficiency (do not need to carry fuel) and high specific impulse. Previous SDIO research led to the invention of the one of the laser powered launch vehicle concept – the Laser Lightcraft concept, currently being tested at the High Energy Laser Test System Facility, White Sands Missile Range, New Mexico. Although the spin-stabilized small scale Lightcraft model (invented by Myrabo) has been flown successfully up to an altitude of 30 meters using a 10 kW pulsed-laser at 10 Hz, many technical issues need to be addressed before an optimized design of the vehicle and its operation can be achieved.

The purpose of this study is to establish the technical ground for modeling the physics of laser powered pulse detonation phenomenon. The principle of the laser power propulsion is that when high-powered laser is focused at a small area near the surface of a thruster, the intense energy causes the electrical breakdown of the working fluid (e.g. air) and forming high speed plasma (known as the inverse Bremsstrahlung, IB, effect). The intense heat and high pressure created in the plasma consequently causes the surrounding to heat up and expand until the thrust producing shock waves are formed. This complex process of gas ionization, increase in radiation absorption and the forming of plasma and shock waves will be investigated in the development of the present numerical model. In the first phase of this study, laser light focusing, radiative absorption and shock wave propagation over the entire pulsed cycle are modeled. The model geometry and test conditions of known benchmark experiments such as those in Myrabo's experiment will be employed in the numerical model validation simulations. The calculated performance data (e.g. coupling coefficients) will be compared to the test data. Plans for the numerical

modeling of the detailed IB effect will also be described in the proposed investigation. The final goal will be the design analysis of the full-scale laser propelled flight vehicle using the present numerical model.

In this study, Engineering Sciences, Inc. has developed a laser powered launch vehicle performance analysis tool based on its in-house flow and radiation codes. UNIC-UNS unstructured-grid flow code and GRADP-UNS unstructured-grid radiation code are two advanced numerical models. Many complex engineering design problems related to fluid dynamics and radiative heat transfer have been solved using these two codes. However, high-temperature thermodynamics and plasma dynamics models still need more developments and benchmark data validations before these two codes can be applied to the design problems of laser powered launch vehicles. The development work shall include transient shock capturing algorithm using unstructured-grid method with dynamic local refinement and coarsening. High temperature thermodynamics and plasma gas dynamics physics shall be modeled and validated. Non-equilibrium radiation model with the effects of gas breakdown and laser energy absorption also needs to be addressed and modeled. These advanced thermodynamics and radiation models will serve as the fundamental building blocks for the development and utilization of the proposed laser powered launch vehicle performance prediction and analysis tool.

As a continuing effort of improving the capability of the laser propulsion modeling analysis tools, general formulations and modeling specifics outlined in the previous section are planned and implemented in the present project. In the first part of this project, a three-temperature model is implemented in the baseline CFD code [1] and tested for the model-A laser lightcraft configuration at 400 J power level. In this study, it is found that the previously employed model for evaluating the Landau-Teller relaxation time scale is not appropriate for three-temperature calculation. A more general model [2] (Peter A. Gnoffo, et al., 1989) is therefore implemented in the present study. Since the three temperatures (namely the heavy-particle temperature, vibrational temperature and electron temperature) are strongly coupled in the transient process, an implicit solution

method is employed to provide stable solutions for this system. The present three-temperature model is described in the following section.

For testing the model performance, the three-temperature model is employed for the thrust performance computations of the model-A laser lightcraft configuration at 200 J, 300 J, 400 J, 600 J and 800 J power levels. The plasma resonant energy conversion factor is fixed at 0.4. Another approach using an idealized model described by C. S. Liu, et al. [3], has been investigated. The goal of this investigation is to replace the assumed plasma resonant energy factor with a better approach. In Liu's model, the absorption coefficient of a plasma sheet beyond resonance frequency can be estimated as a function of incoming ray angles and a critical length scale. Preliminary results of coupling coefficient calculation using this model have shown under prediction in vehicle thrust. This indicates that the conversion factor predicted is on the low side. The coupling coefficient predicted using Liu's model is too low compared to the test data (about 19.5% for the 400 J case). It is concluded that Liu's model, which is derived using many simplified assumptions, is not general enough for all laser incident angles. The low absorption level predicted using this model is not acceptable to be incorporated in the current method. Therefore, it is decided to stay with the current fixed 40% absorption rate for plasma resonance.

Extension of the computational model to 3-D operation conditions using parallel computing methods is also completed in the present effort. The 3-D model involves more complicated general ray tracing and boundary reflection conditions for the radiation model. Parallel algorithms for the general ray tracing and radiation solution are implemented in the present analysis tool. Some observations and recommendations for the air-breathing and rocket mode applications are discussed.

COMPUTATIONAL FLUID DYNAMICS MODEL

Governing Equations

For The Continuity, Navier-Stokes and Energy (Total Enthalpy) Equations, can be written in a Cartesian tensor form:

$$\frac{\partial \rho}{\partial t} + \frac{\partial}{\partial x_j} (\rho u_j) = 0 \quad (1)$$

$$\frac{\partial \rho u_i}{\partial t} + \frac{\partial}{\partial x_j} (\rho u_j u_i) = -\frac{\partial p}{\partial x_i} + \frac{\partial \tau_{ij}}{\partial x_j} \quad (2)$$

$$\frac{\partial \rho H}{\partial t} + \frac{\partial}{\partial x_j} (\rho u_j H) = \frac{\partial p}{\partial t} + Q_{ec} + Q_v + \frac{\partial}{\partial x_j} \left(\frac{\mu}{P_r} \nabla H \right) + \frac{\partial}{\partial x_j} \left(\left(1 - \frac{\mu}{P_r} \right) \nabla (V^2 / 2) \right) \quad (3)$$

$$\frac{\partial}{\partial t} \left(\frac{2}{3} k_b n_e T_e \right) + \frac{\partial}{\partial x_j} \left(\frac{2}{3} k_b n_e T_e u_j \right) = \frac{\partial}{\partial x_j} \left(\lambda_e \frac{\partial T_e}{\partial x_j} \right) + Q_r - Q_{ec} \quad (4)$$

where ρ is the fluid density, u_i is the i^{th} Cartesian component of the velocity, p is the static pressure, μ is the fluid viscosity, P_r is the Prandtl number, H is the gas total enthalpy and V stands for the sum of velocity squared. In Eq. (4), k_b , n_e , T_e , λ_e , Q_r , Q_v and Q_{ec} are the Boltzmann's constant, electron number density, electron temperature, electron thermal conductivity, radiative heat source from laser absorption and radiative transfer, vibrational-translation energy transfer source term, and the energy transfer due to electron/particle elastic collisions, respectively. The shear stress τ_{ij} can be expressed as:

$$\tau_{ij} = (\mu + \mu_t) \left(\frac{\partial u_i}{\partial x_j} + \frac{\partial u_j}{\partial x_i} - \frac{2}{3} \frac{\partial u_k}{\partial x_k} \delta_{ij} \right) - \frac{2}{3} \rho k \delta_{ij}$$

The species conservation equation is expressed as:

$$\frac{\partial \rho Y_i}{\partial t} + \frac{\partial}{\partial x_j} (\rho u_j Y_i) = \frac{\partial}{\partial x_j} \left[\left(\rho D + \frac{\mu_t}{\sigma_Y} \right) \frac{\partial Y_i}{\partial x_j} \right] + \dot{\omega}_i$$

where Y_i is the i^{th} species mass fraction, D is the mass diffusivity, σ_Y is the turbulent Schmidt number, and $\dot{\omega}_i$ is the chemical reaction rate for species i respectively.

Vibrational Energy Equation

For high temperature gas flows, thermal non-equilibrium state may be important. In Landau and Teller's derivation, a master equation is employed to describe the evolution of the population of quantum level N_i . This master equation is written as:

$$\frac{dN_i}{dt} = N \sum_{j=0}^{I_{\max}} K_{j \rightarrow i} N_j - N \sum_{j=0}^{I_{\max}} K_{i \rightarrow j} N_i; \quad i = 0, 1, 2, \dots, I_{\max}$$

Results from the quantum mechanical solution of the harmonic oscillator are used to relate the various quantum transition rates to one another, and then the master equation may be summed over all quantum states to arrive at the Landau-Teller equation:

$$\frac{D \rho e_v}{Dt} = \frac{\partial}{\partial x_i} \left(k_v \frac{\partial T_v}{\partial x_i} \right) + \rho \frac{e_v^{eq}(T_i) - e_v}{\tau_{LT}} \approx \frac{\partial}{\partial x_i} \left(k_v \frac{\partial T_v}{\partial x_i} \right) + \rho \frac{C_{v,v}(T - T_v)}{\tau_{LT}}$$

where ρ , e_v , e_v^{eq} and τ_{LT} represent the gas density, vibrational energy, effective (equilibrium) vibrational energy and the vibrational-translational relaxation time scale respectively. An empirical expression (to be discussed in the next section) is used to model the Landau-Teller relaxation time scale.

As discussed by Gnoffo (1989), the vibrational-translation energy relaxation time scale can be evaluated using the following equation

$$\tau_{LT} = \frac{\sum_{s=mol.} \rho_s / M_s}{\sum_{s=mol.} \rho_s / M_s < \tau_s >}$$

and

$$< \tau_s > = \tau_s^{MW} + \tau_s^P$$

$$\tau_s^P = \left(\sigma_s \bar{c}_s n_s \right)^{-1}$$

$$\bar{c}_s = \left(8k_b T / \pi m_s \right)^{1/2}$$

$$\tau_s^{MW} = \frac{\sum_{j=1}^{10} n_j \exp \left[A_s \left(T^{-1/3} - 0.015 \mu_{sj}^{1/4} \right) - 18.42 \right]}{p \sum_{j=1}^{10} n_j}$$

where subscript s represents the participating species (only diatomic species are involved here). σ , n , m and μ denote the effective cross section, species number density, species unit mass and reduced molecular weight, respectively. The correlation constant, A_s , has different values for each participating species. They are given in the table below.

s	Ms	As
N2	28	220
O2	32	129
N	14	0
O	16	0
NO	30	168
N+	14	0
O+	16	0
N2+	28	220
O2+	32	129
NO+	30	168
e-	.0005486	0

BENCHMARK TEST CASES STUDY

400 J 30- μ sec Pulse Width Test Case

The test conditions of this case are listed below. The laser ignition procedure of the baseline model is used. A pie-area of spark ignition region is assigned initially. It is assumed that 15 percent of the laser energy is absorbed and converted into thermal energy during this spark ignition time period. When laser absorption efficiency reaches 15 percent, the spark ignition process will be terminated and normal laser absorption mode would remain. After this point, all absorbed laser energy is used as the energy source for the electron energy equation. Subsequent energy transfer to heavy particle and vibrational mode is solved by the coupled three-temperature energy equation. When the electron number density reaches the threshold value beyond which plasma resonance would occur, 30 percent energy conversion rate is assumed for the present model. More rigorous model should be employed to model the energy conversion for plasma resonance. The flowfield solutions at two time levels are shown in the following figures (Figures 1 to 4). The coupling coefficient time histories of two-temperature and three-temperature models are also compared in Figure 5.

Model Conditions:

- Vehicle Configuration Model-A of Myrabo's Flight Tests (Closed Air Inlet)
- Pulsed Laser at 10 Hz and 30 μ s Pulse Width
- Laser Energy Level = 400 J
- Total Number of Mesh Elements = 16,870
- Assuming Axisymmetric Model
- Assumed Energy Absorption Scheme
- Testing the Predictions of Detonation Wave Propagation and Vehicle Thrust Calculation

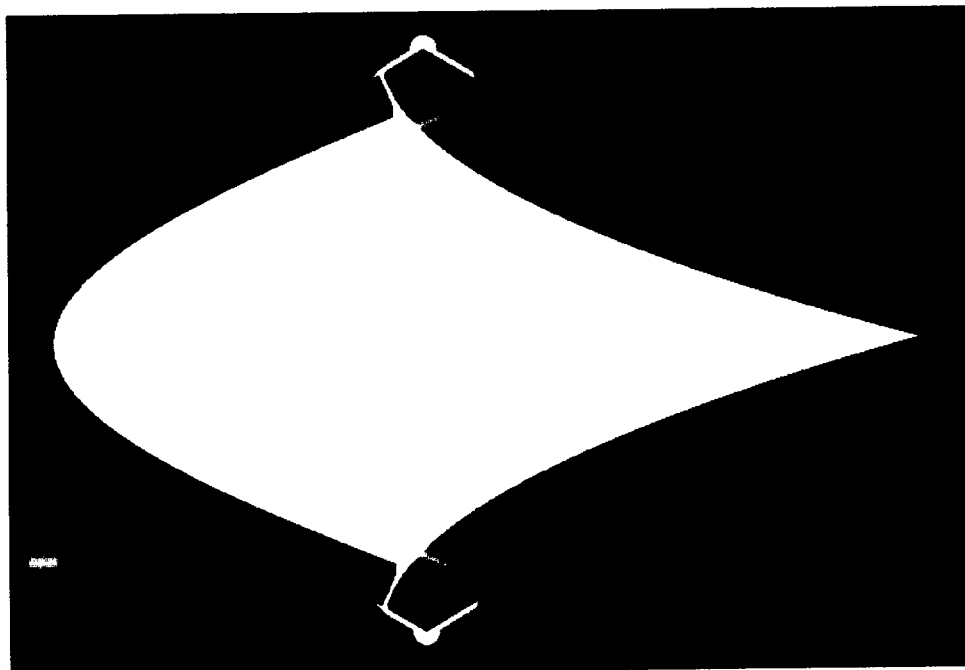


Figure 1. Pressure contours (ATM) at 300 time steps.

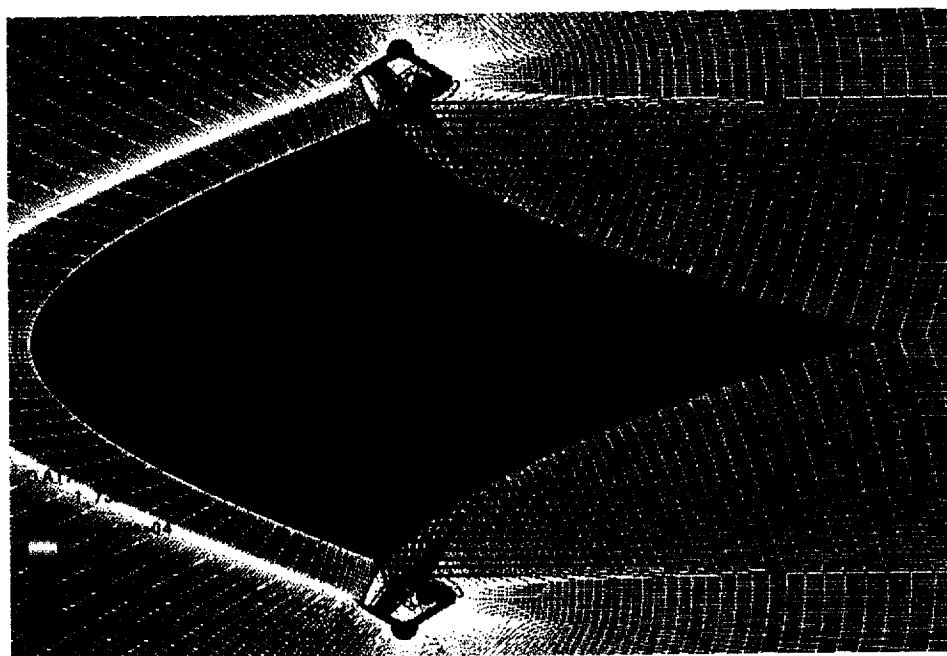


Figure 2. Temperature contours (K) at 300 time steps.

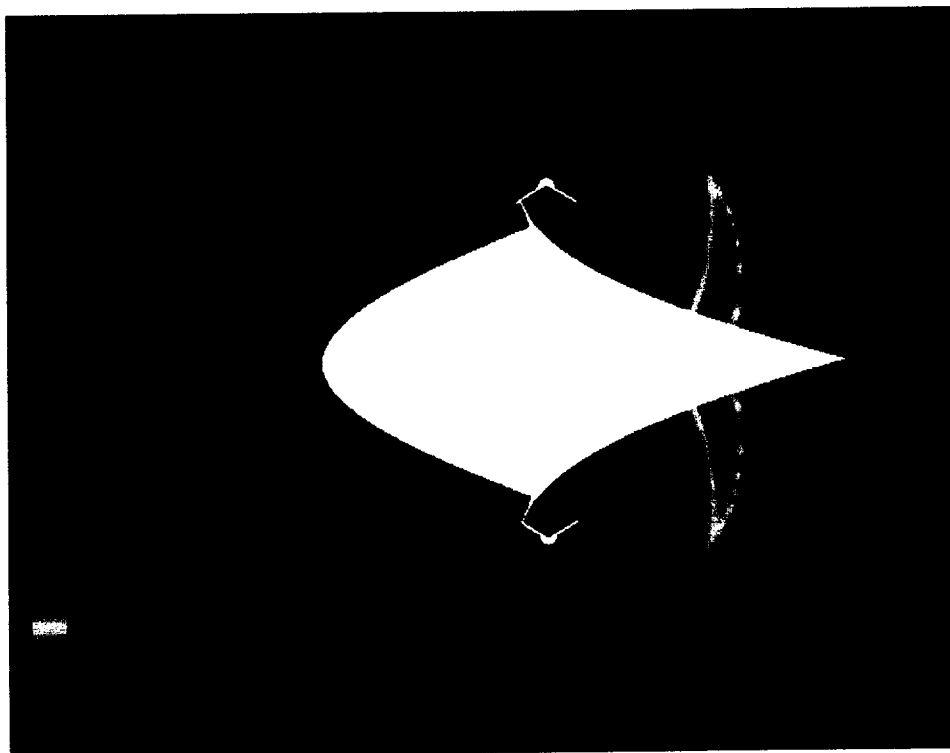


Figure 3. Pressure contours (ATM) at 1170 time step.

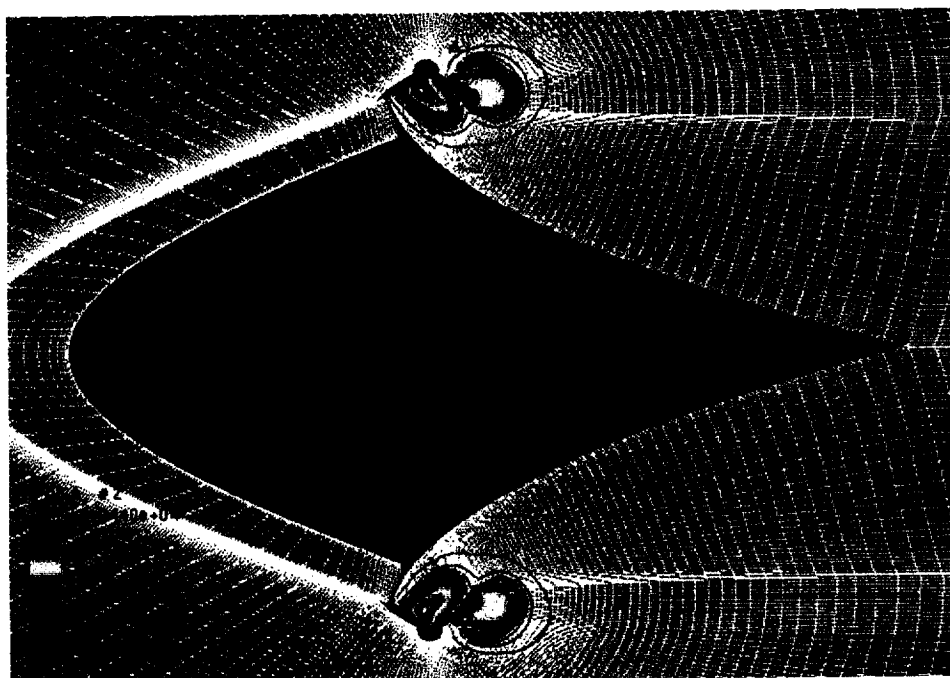


Figure 4. Temperature contours (K) at 1170 time step.

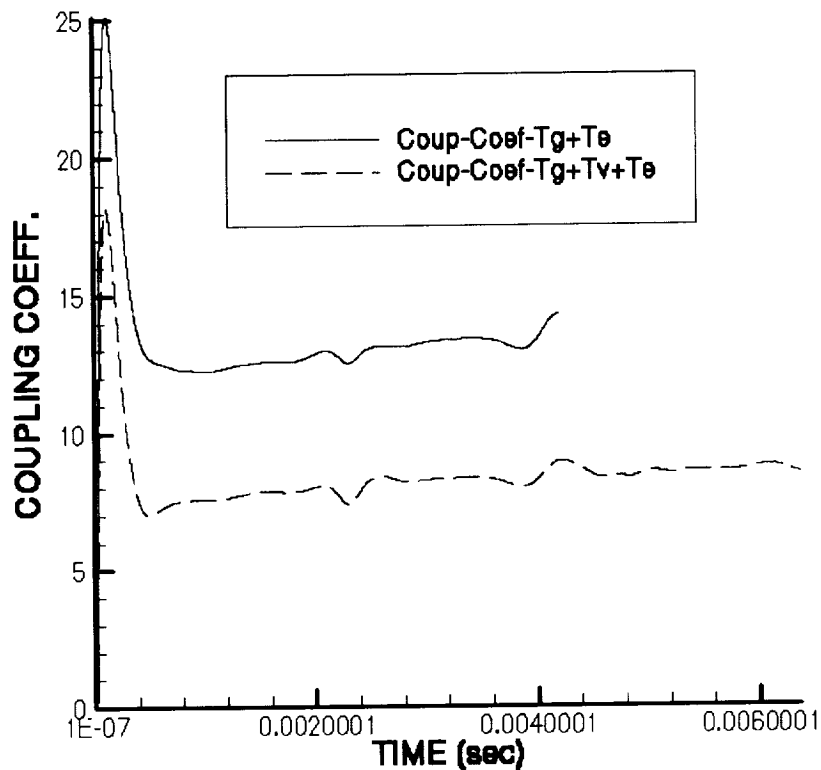


Figure 5. Comparisons of coupling coefficient time histories for two-temperature and three-temperature models.

This three-temperature model, with 30 percent absorption rate assumed for the resonant plasma, under-predicts the coupling coefficient as shown in Figure 5. The result of the two-temperature model is very close to the measured data. This is expected since the assumed energy conversion rate in the plasma resonance regime of 30 percent was tuned based on the two-temperature model. A higher energy conservation rate will give good predictions for the current three-temperature model. A more rigorous model will be employed to eliminate this energy conversion assumption.

Resonant Energy Conversion Factor Study

Model-A lightcraft thrust coupling coefficients for 400 J, 600 J and 800 J power levels have been predicted using the present 3 temperature computational

model. The computation starts with a small time step size, $1.0\text{E-}7$ sec, and steps up to larger time steps within the laser pulse width of 30 micro-sec. Small time step at the start is necessary for stable solution due to high concentration of laser energy near the focus. A typical case takes about 8000 time steps to produce a nearly constant integrated coupling coefficient. The grid size for this model is 17,184. It takes around 3 days run time to obtain a solution for each case. Figure 6 shows the coupling coefficient comparisons for 400 J laser power level.

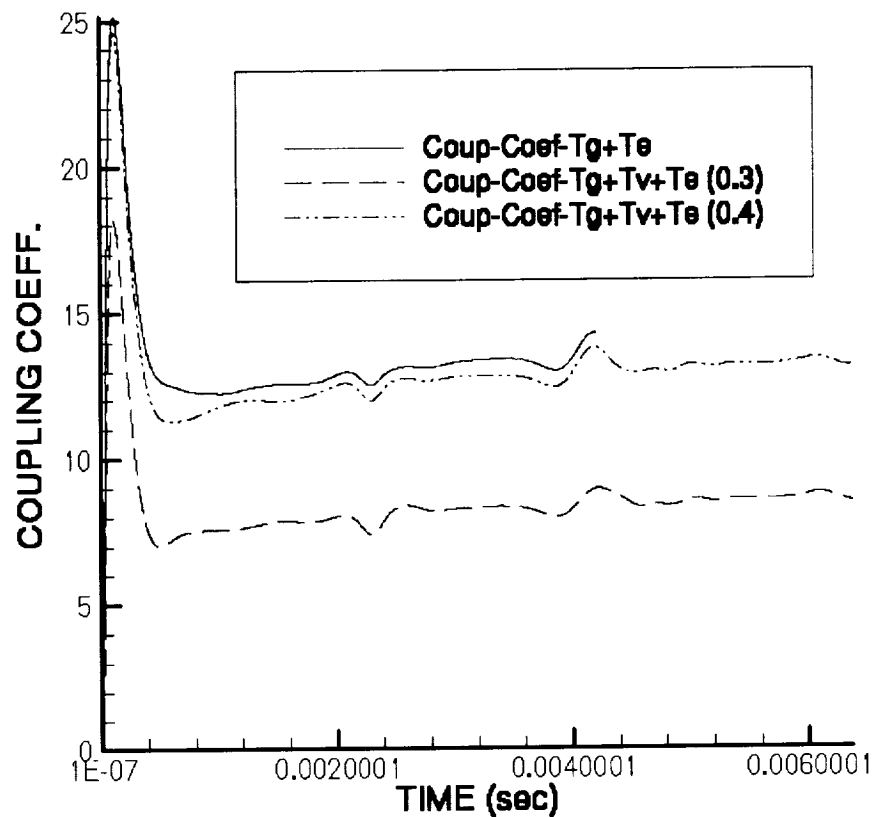


Figure 6. Comparisons of coupling coefficient time histories for two-temperature and three-temperature models for 400 J laser.

Figures 7 and 8 show the predicted coupling coefficients for 600 J and 800 J laser power level.

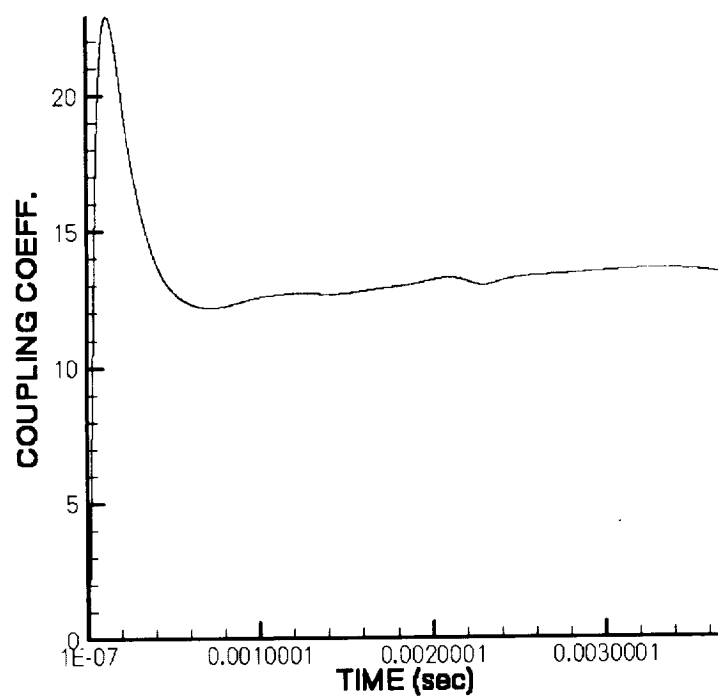


Figure 7. Predicted coupling coefficient for 600 J laser power.

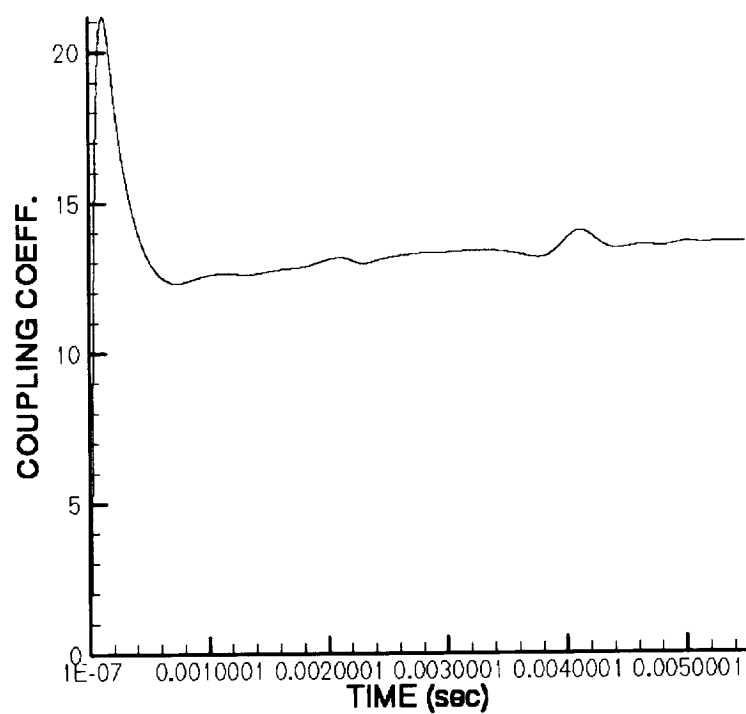


Figure 8. Predicted coupling coefficient for 800 J laser power.

The present three-temperature model over-predicts the coupling coefficient slightly. Lower coupling coefficient prediction is expected as non-equilibrium plasma radiation model is considered in the computation.

Study of All Power Levels

Model-A lightcraft thrust coupling coefficients for 200 J, 300 J, 400 J, 600 J and 800 J power levels have been predicted using the present 3 temperature computational model. The computation starts with a small time step size, $1.0\text{E-}7$ sec, and steps up to larger time steps beyond the laser pulse width of 30 micro-sec. Small time step at the start is necessary for better time resolution and solution stability due to high concentration of laser energy near the focus. A typical case takes about 8000 time steps to produce a nearly constant integrated coupling coefficient. The grid size for this model is 17,184. It takes around 3 days run time to obtain a solution for each case using one processor. Figure 9 shows the coupling coefficient comparisons for the 5 laser power levels.

In the present spark ignition modeling, all spark energy (which is assumed to be 15% of the available beam power) is used as the source of the heavy gas energy equation. Within the spark time period, the one-temperature model is used. Vibrational and electron temperatures are then assigned to be the same level as the heavy gas temperature after every time step. This treatment is found to create inconsistent energy source budget when different initial time step size is used. The three-temperature model seems to produce consistent results for different initial time step sizes. This approach will be further investigated to confirm that it will be the better alternative than the present spark ignition model.

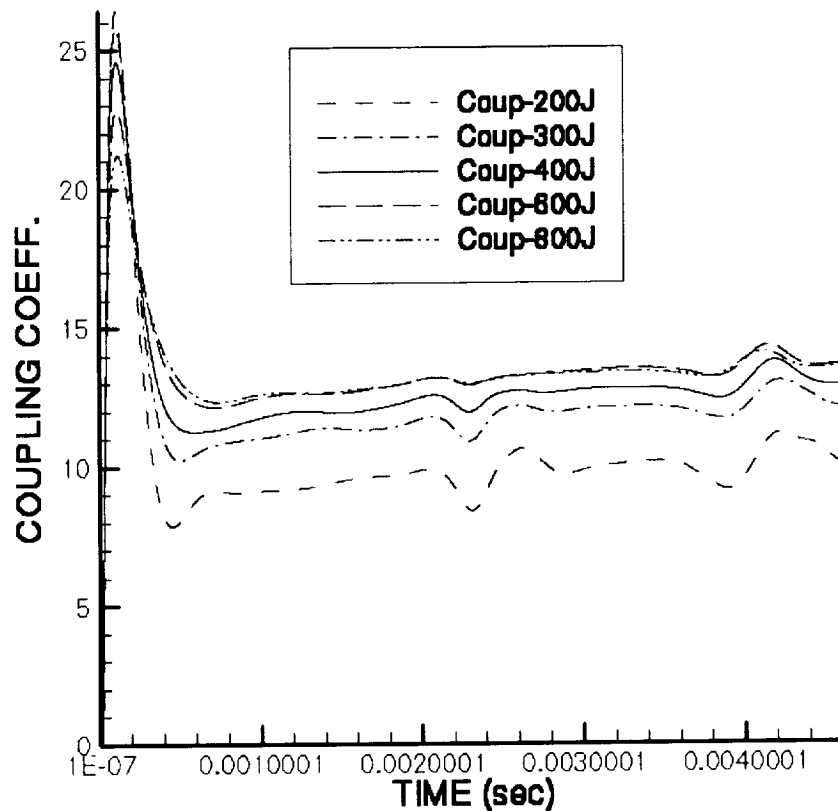


Figure 9. Comparisons of coupling coefficient time histories for 5 laser power levels.

Parallel and 3-D Ray Tracing Radiation Model

a. Laser Beam Ray Tracing Using Parallel Computation

Laser radiation absorption is one of the most important phenomena in the analysis of laser propelled lightcraft and its modeling is based on the geometric optics in the present study. In the geometric optics, the laser beam is assumed to consist of a finite number of individual laser rays, each ray is then traced until it is totally absorbed by a gas or surface element. In the previous analysis, ray tracing for the laser beam was implemented on a sequence computer. In the current period of the project, a parallel algorithm has been developed to extend the ray tracing calculation of laser beam in parallel computation.

The ray tracing is a time sequence process and its implementation in a sequence computer is straightforward through tracing a ray volume by volume until a boundary is reached. However, when multiple computers are used in a ray tracing process, its implementation becomes different since only one computer (not all computers) is involved in an actual ray tracing calculation while other computers are essentially idle. To implement a parallel algorithm, an iterative computation procedure is developed in the present computer program. Each iteration involves ray tracing in a single subdomain associated with a specific computer. In a specific iteration, all information required in the ray tracing is passed from the previous iteration. A detailed implementation procedure is provided below.

- (1) Decompose the computational domain by the METIS software. Each subdomain is then assigned to a specific computer processor.
- (2) Assign the ray tracing *flag* values to all the computer processor. The value of 1 means the ray tracing takes place in the current processor.
- (3) Decide the subdomain and the corresponding processor index number from which each ray starts for a ray tracing calculation. The value of the ray tracing *flag* is set to be unity for this processor.
- (4) Start the ray tracing in the processor with *flag*=1 while other processors are idle. The ray tracing calculation involves tracing a ray volume by volume in the designated subdomain until a boundary element is reach.
- (5) If the boundary element is a zonal boundary, the information on the intersection point is saved and passed to its adjoint subdomain by calling the PVM library. The ray tracing *flag* becomes unity for the processor corresponding to this adjoint subdomain. Then, the calculation enters into the next iteration by repeating step (4). If the boundary element is reflective surface, the ray tracing continues in the same subdomain after the ray reflection. If the boundary element is other surface, the ray tracing ends here and the calculation move on for the next ray.

In order to check the accuracy and efficiency of the developed parallel algorithm, a laser propelled lightcraft problem with the laser power equal to 370 J has been examined for three cases with processor number N_p equal to 1, 2, and 6, respectively. Figure 10 demonstrates the corresponding coupling coefficient distributions. It is clear that the results from different processor number are very close. This confirms that the present parallel implementation is correct. In addition, the parallel performance is also investigated and the speedups for different N_p are found to be close to the ideal speedup.

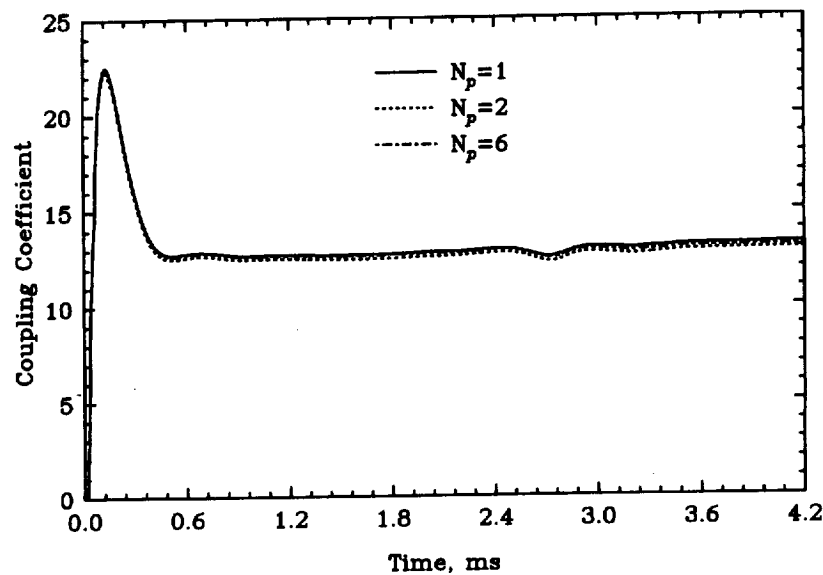


Figure 10. Comparison of the coupling coefficient distributions for different processor number.

b. Laser Beam Ray Tracing in 3-D Geometry

In the previous analysis, the ray tracing calculation was only applied for a 2-D geometry. In the current period of the project, the computer code has been developed to extend the ray tracing calculation for a 3-D geometry. In the 2-D ray tracing code, the laser ray tracing conditions are easily provided in the input data file *unic.inp*. However, the ray tracing conditions for a 3-D geometry becomes much more involved. Thus a special subroutine has been developed to

implement these conditions in the present 3-D study. In this subroutine, the geometrical and laser intensity information for the input laser imprint is provided. The imprint area is then discretized into many small surfaces. Each of these surfaces is associated with a laser ray. It is noted that the discretization of the laser imprint area has nothing to do with the computational grid used for the laser lightcraft. To connect these two grids, the imprint area grid along with the laser ray intensity is mapped on the boundary of the computational grid. With this mapping, the starting location and power intensity for each ray on the computational grid are known and the ray tracing calculation can begin. Similar to a 2-D geometry, the ray tracing in a 3-D geometry involves tracing a ray volume by volume until a boundary is reached.

In order to validate the present 3-D ray tracing code, a 3-D problem has been constructed by rotating the existing 2-D grid over 45° . The laser imprint area considered is of square shape. Due to the symmetry, only a eighth of the square is used. The imprint area is divided into 30×20 grid representing 600 laser-beam rays. By analyzing all the intersection points of each ray in the computational domain, the 3-D ray tracing has been found to be correct. With the validation of 3-D ray tracing calculation, a 3-D modeling of laser propelled lightcraft becomes possible and it has been tried in a hypothetical 3-D problem.

Air Breathing and Rocket Mode Effects

In practical design of laser powered launch vehicles, the performance of air supply through intake passages may affect the overall thrust performance of the vehicle. At very high altitudes, it will be necessary to switch to rocket mode that the propellant carried in the vehicle are injected and detonated for each pulsed laser cycle. For numerical analysis for the air breathing or rocket modes, the same physical models can be applied. What needs to be included in the model is the inclusion of air intake passage control and injection scheme arrangement. It is envisioned that the present model can be directly applied to these conditions without any problem.

CONCLUSIONS

In the present research project, a comprehensive computational model has been developed for the prediction of laser supported propulsion system that involved thermal, chemical and radiative non-equilibrium flow physics. The model-A laser lightcraft design has been analyzed for a series of laser power inputs. The predicted thrust coupling coefficients show good agreement with the measured data. Extension of this model to 3-D and parallel computing conditions, which involves a general radiative ray-tracing scheme, has been completed and tested. More studies are needed to determine the plasma-resonance energy conversion factor, which seems to be of major contributions to the integrated thrust coupling coefficients.

REFERENCES

1. Wang, T. S., Chen, Y. S., Liu, J., Myrabo, L. N., and Mead, F. B., Jr., "Performance Modeling of an Experimental Laser Propelled Lightcraft," 31st AIAA Plasmadynamics and Lasers Conference, 19-22 June 2000, Denver, CO.
2. Gnoffo, Peter A., Gupta, Roop N., and Shinn, Judy L., "Conservation Equations and Physical Models for Hypersonic Air Flows in Thermal and Chemical Nonequilibrium," NASA TP-2867, 1989
3. Liu, C. S. and Tripathi, V. K., Interaction of Electromagnetic Waves with Electron Beams and Plasmas, World Scientific Publishing Co. Pte. Ltd., 1994.

REPORT DOCUMENTATION PAGE			Form Approved OMB No. 0704-0188	
Public reporting burden for this collection of information is estimated to average 1 hour per response, including the time for reviewing instructions, searching existing data sources, gathering and maintaining the data needed, and completing and reviewing the collection of information. Send comments regarding this burden estimate or any other aspect of this collection of information, including suggestions for reducing this burden, to Washington Headquarters Services, Directorate for Information Operations and Reports, 1215 Jefferson Davis Highway, Suite 1204, Arlington, Va 22202-4302, and to the Office of Management and Budget, Paperwork Reduction Project (0704-0188), Washington, DC 20503.				
1. AGENCY USE ONLY (Leave Blank)		2. REPORT DATE May 31, 2001		3. REPORT TYPE AND DATES COVERED Final Technical Report
4. TITLE AND SUBTITLE LASER POWERED LAUNCH VEHICLE PERFORMANCE ANALYSES			5. FUNDING NUMBERS H-32385D	
6. AUTHOR(S) Yen-Sen Chen and Jiwen Liu				
7. PERFORMING ORGANIZATION NAME(S) AND ADDRESS(ES) Engineering Sciences, Inc. 1900 Golf Road, Suite D Huntsville, AL 35802			8. PERFORMING ORGANIZATION REPORT NUMBERS	
9. SPONSORING/MONITORING AGENCY NAME(S) AND ADDRESS(ES) George C. Marshall Space Flight Center Marshall Space Flight Center, AL 35812			10. SPONSORING/MONITORING AGENCY REPORT NUMBER	
11. SUPPLEMENTARY NOTES Ten-See Wang / Technical Monitor				
12a. DISTRIBUTION/AVAILABILITY STATEMENT			12b. DISTRIBUTION CODE	
13. ABSTRACT (Maximum 200 words) <p>The purpose of this study is to establish the technical ground for modeling the physics of laser powered pulse detonation phenomenon. Laser powered propulsion systems involve complex fluid dynamics, thermodynamics and radiative transfer processes. Successful predictions of the performance of laser powered launch vehicle concepts depend on the sophisticated models that reflects the underlying flow physics including the laser ray tracing the focusing, inverse Bremsstrahlung (IB) effects, finite-rate air chemistry, thermal non-equilibrium, plasma radiation and detonation wave propagation, etc. The proposed work will extend the base-line numerical model to an efficient design analysis tool. The proposed model is suitable for 3-D analysis using parallel computing methods.</p>				
14. SUBJECT TERMS Laser Propulsion, Detonation Wave Engine, CFD Model			15. NUMBER OF PAGES 21	
			16. PRICE CODE	
17. SECURITY CLASSIFICATION unclassified	18. SECURITY CLASSIFICATION OF THIS PAGE unclassified	19. SECURITY CLASSIFICATION OF ABSTRACT unclassified	20. LIMITATION OF ABSTRACT unlimited	

